A simple 1-dimensional, climate based dissolved oxygen model for the central basin of Lake Erie

Daniel K. Rucinski [a,b,*], Dmitry Beletsky [b,c], Joseph V. DePinto [a,b], David J. Schwab [d], Donald Scavia [b,e]

[a] LimnoTech, 501 Avis Drive, Ann Arbor, MI 48108, USA
[b] School of Natural Resources and Environment, University of Michigan, 440 Church Street, Ann Arbor, MI 48109, USA
[c] Cooperative Institute for Limnology and Ecosystem Research, 440 Church Street, Ann Arbor, MI 48109, USA
[d] NOAA Great Lakes Environmental Research Laboratory, 4840 S. State Rd., Ann Arbor, MI 48108, USA
[e] Graham Environmental Sustainability Institute, University of Michigan, Ann Arbor, MI 48109, USA

ARTICLE INFO

ABSTRACT

A linked 1-dimensional thermal-dissolved oxygen model was developed and applied in the central basin of Lake Erie. The model was used to quantify the relative contribution of meteorological forcings versus the decomposition of hypolimnetic organic carbon on dissolved oxygen. The model computes daily vertical profiles of temperature, mixing, and dissolved oxygen for the period 1987–2005. Model calibration resulted in good agreement with observations of the thermal structure and oxygen concentrations throughout the period of study. The only calibration parameter, water column oxygen demand (WCOD), varied significantly across years. No significant relationships were found between these rates and the thermal properties; however, there was a significant correlation with soluble reactive phosphorus loading. These results indicate that climate variability alone, expressed as changes in thermal structure, does not account for the inter-annual variation in hypoxia. Rather, variation in the production of organic matter is a dominant driver, and this appears to have been responsive to changes in phosphorus loads.

Introduction

Historically, Lake Erie has been subject to significant cultural eutrophication. Excess phosphorus (P) entering the lake primarily from agricultural runoff and point source discharges (Dolan, 1993) have resulted in hazardous and nuisance algal blooms, poor water clarity, and summer hypoxia in the hypolimnion of the central basin. In response to concern about the consequences of eutrophication, the governments of the U.S. and Canada, largely through the auspices of the Great Lakes Water Quality Agreement (GLWQA, 1978), implemented a program of P load reduction that was unprecedented for any region of the world (DePinto et al., 1986). A combination of point and non-point phosphorus load reductions achieved the target load of 11,000 metric tonnes per year and the response of the lake was rapid, profound, and close to that predicted by models (Bertram, 1993; Di Toro et al., 1987; Makarewicz, 1993). Despite this apparent success at reversing eutrophication, periodic hypoxia (dissolved oxygen < 2 mg L^{-1}) in the hypolimnion of the central basin of Lake Erie persisted, and more recently enlarged and reemerged as a potential hazard to ecosystem health (Burns et al., 2005). Several natural and anthropogenic factors are at least jointly responsible for causing this resurgence. These include

changes in climate and hydrology (Blumberg and Di Toro, 1990; Diaz, 2001; Atkinson et al., 1999; Lam et al., 1987), invasion of benthic filter feeders (e.g., zebra and quagga mussels; Woynarovich, 1961), and increased agricultural loading (Richards, 2006).

Climate change is expected to result in warmer temperatures, loss of ice cover, and decreased lake levels in many areas (Bates et al., 2008). The warming climate could have considerable implications on the Lake Erie's stratification, and modeling studies have suggested this can impact dissolved oxygen (Blumberg and Di Toro, 1990; Fang and Stefan, 1997; Lehman, 2002). The timing and strength of stratification is a function of climate (i.e., atmospheric heating, wind mixing). Early and hot summers can lead to longer stratified periods and deeper thermoclines, resulting in a smaller reservoir of bottom-water oxygen and prolonged isolation from surface mixing. Additionally, shorter term meteorological conditions have been shown to have an impact on the rate of oxygen depletion via enhanced mixing from storms (Lam et al., 1987). Hydrology is also a function of climate, and increasing wetter periods with more intense and frequent winter and spring storms (Croley, 1990; Lofgren et al., 2002) can lead to increased runoff and the associated nutrient loads that stimulate phytoplankton growth and thus significantly impact dissolved oxygen conditions (Edwards et al., 2005; El-Shaarawi, 1987). Because these processes can vary considerably from year to year, the extent to which they contribute to hypoxia is also variable. The primary purpose of this paper is to describe a modeling analysis performed to quantify the

* Corresponding author. School of Natural Resources and Environment, University of Michigan, 440 Church Street, Ann Arbor, MI 48109, USA.
E-mail address: drucinski@limno.com (D.K. Rucinski).

relative effects climate has had on inter-annual variability in dissolved oxygen dynamics in the central basin of Lake Erie. We do this by isolating climate effects on thermal structure and exploring the resulting ability of the model to reproduce observations in hypoxia structure and formation between 1987 and 2005, a period capturing dramatic changes in the ecosystem of Lake Erie.

Study area

Lake Erie is the smallest and shallowest of the Laurentian Great Lakes and it has the highest ratio of drainage area to surface area. Its drainage basin is the most populated and it contains the highest proportion of agricultural lands and several major urban areas. These physical characteristics and land use can lead to excessive nutrients entering the lake (Richards, 2006; Richards and Baker, 2002).

The morphology of Lake Erie is also conducive to eutrophication and has been shown to influence oxygen depletion (Charlton, 1980b). The lake has three distinct basins (Fig. 1). The western basin is the shallowest, and rarely stratifies thermally, preventing low oxygen conditions from developing in bottom waters. Conversely, the eastern basin is very deep, and does experience strong stratification. However, its hypolimnion is large enough that oxygen resources are rarely depleted. The central basin, however, is transitional with an intermediate depth, allowing it to stratify annually, but with a relatively thin hypolimnion. It also receives a significant load of nutrients from the western basin. Thermal stratification inhibits oxygen transfer to bottom waters, and decomposition of organic matter decreases oxygen conditions. As a result, the central basin is generally the only part of Lake Erie to experience hypoxia (Bertram, 1993).

Modeling

Modeling objective and approach

Our objective was to investigate the inter-annual variability in dissolved oxygen dynamics in central basin of Lake Erie, and to assess the extent to which that variability is caused by variability of climate-driven mixing and temperature regimes. To accomplish this, a one-dimensional, linked thermal budget and dissolved oxygen model was developed. The dissolved oxygen model is a considerable simplification of the biological processes in the lake because the model was intended to focus on the effects of vertical stratification and mixing dynamics.

Thermal model

Previously, a 1D model with a Richardson number dependent vertical diffusivity coefficient was developed to simulate thermal structure of Lake Erie in 1967–1982 (Lam and Schertzer, 1987). The physical model used in this study is based on a 1D version of the Princeton Ocean Model (Blumberg and Mellor, 1987) developed for Lake Michigan applications (Chen et al., 2002). The 1D model uses a two-equation Mellor-Yamada turbulence model for vertical diffusivity
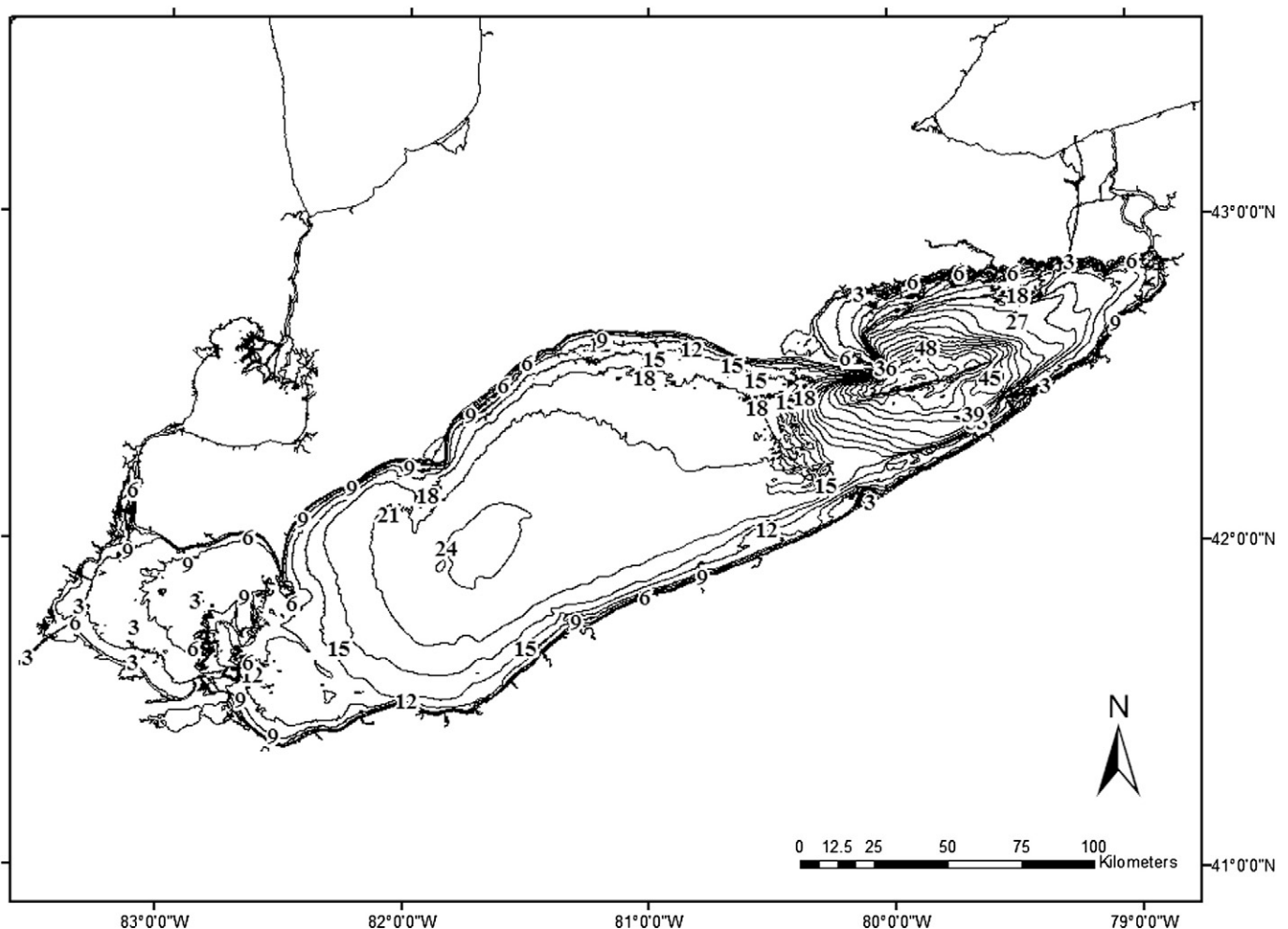

Fig. 1. Morphology of Lake Erie.

(Mellor and Yamada, 1982) and is fully described in Mellor (2001). Model depth is 24 m with 48 layers of 0.5 m each.

Meteorological forcing (momentum and heat fluxes) was calculated using bulk methods described in Beletsky and Schwab (2001) and was based on hourly surface observations from the Cleveland, Ohio airport during 1988–2005. Archived data for wind speed, dew point, and cloud cover were obtained from the NOAA National Climatic Data Center. The airport data were adjusted to be more
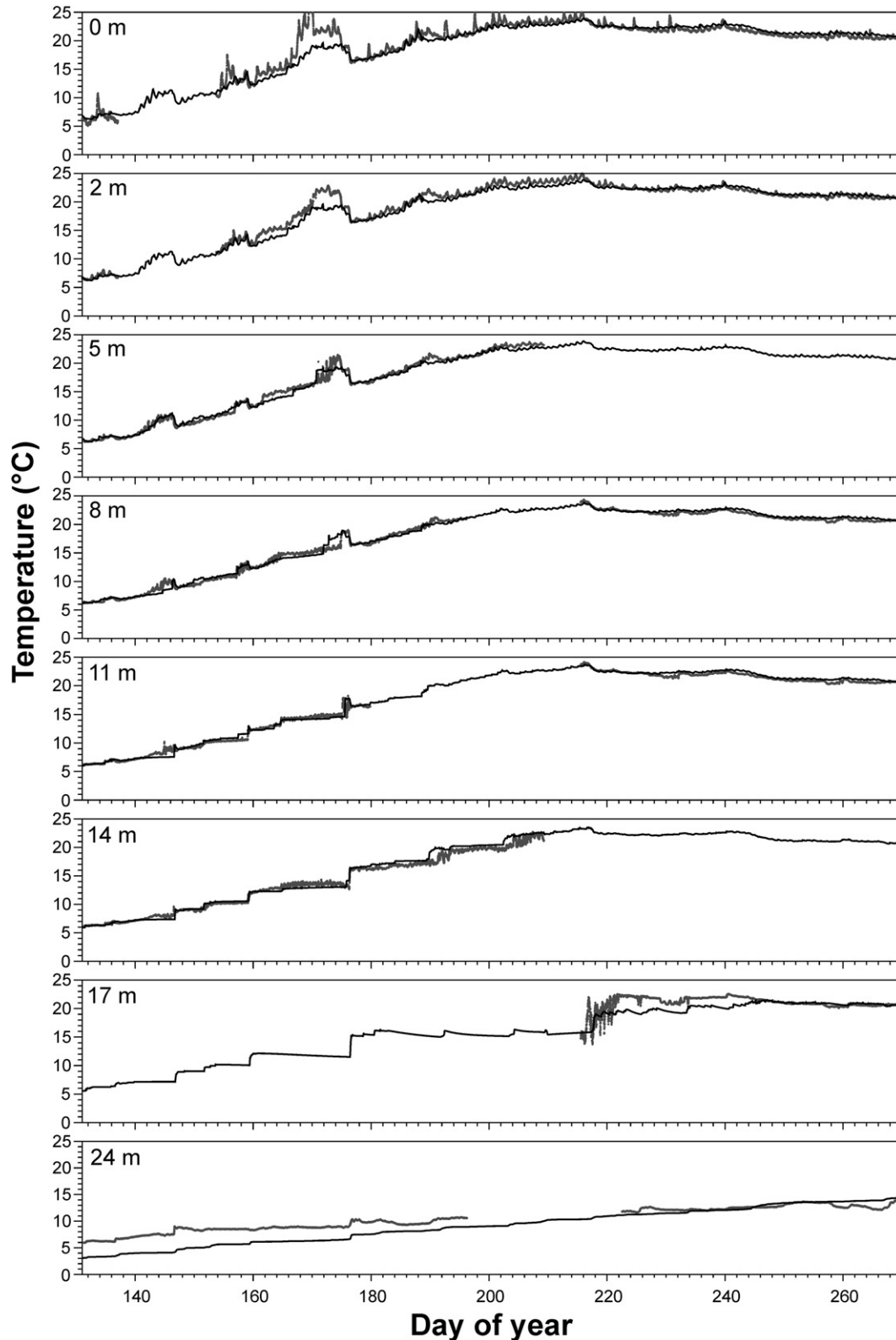

Fig. 2. Time-series of modeled (black) versus observed (gray) temperature at various depths in central Lake Erie in 1994.
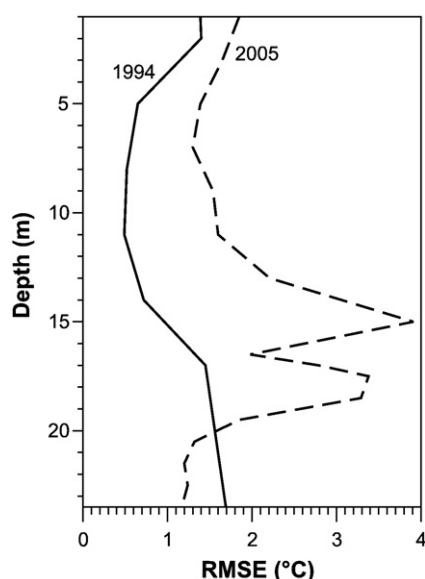
Fig. 3. Comparison of thermal model error (RMSE) with depth.

Fig. 4. Conceptual diagram of dissolved oxygen model.

representative of overlake conditions using the empirical relationships used operationally in the Great Lakes Coastal Forecasting System (Schwab and Bedford, 1999).

The model was calibrated with 1994 temperature observations in central Lake Erie (Fig. 2). Adjustments to increase mixed layer depth consisted of increase of a coefficient B in the surface wave breaking parameterization (Mellor and Blumberg, 2004), to a value of 8×10^{-5}, and addition of internal wave breaking parameterization $\sim C \times N^2$ (where N — is Brunt–Vaisala frequency). The latter process was shown to be important for accurate mixed layer depth simulation (Kantha and Clayson, 1994). Without including this process, the model produced too shallow a mixed layer. A value of 2.8 for coefficient C provided the best match of modeled temperature with 1994 observations. Decreasing the internal time step to 1 min led to slight improvement in model results as well. We also modified the short wave radiation model used in POM (after Paulson and Simpson, 1977) in accordance with results of McCormick and Meadows (1988) obtained for Lake Erie. The incoming short wave radiation is split 55/45 between infra-red and visual bands with extinction coefficients of $2.85 \, m^{-1}$ and $0.28 \, m^{-1}$, respectively. Overall, model errors (RMSE) were between 0.5 and 1.7 °C with maximum errors occurring in the thermocline, below 17 m (Fig. 3).

Dissolved oxygen model

The dissolved oxygen sub-model consists of a coupled set of differential mass balance equations, one for each of the 48 model segments. This system of eq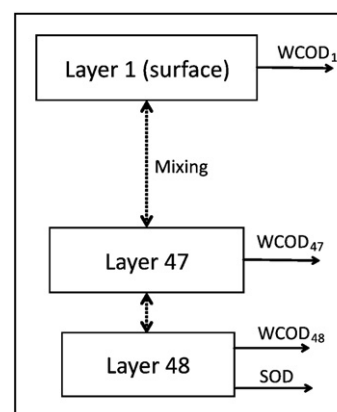uations was solved numerically using an Euler integration scheme. The mass balance equation for the nth segment is shown in Eq. (1).

$$\frac{\partial DO_n}{\partial t} = -WCOD_n + \frac{E_{n-1,n} A_n}{z \, V_n}(DO_{n-1} - DO_n) \tag{1}$$
$$+ \frac{E_{n+1,n} A_n}{z \, V_n}(DO_{n+1} - DO_n) + SOD_n$$

Where

DO_n Dissolved oxygen (mg L^{-1}) in model segment n
$WCOD_n$ Water column oxygen demand (mg L^{-1} d^{-1}) in model segment n
SOD_n Sediment oxygen demand (g m^{-2} d^{-1}) in bottom layer (0 in other layers)
$E_{n-1,n}$ Turbulent dispersion coefficient (m^2 s^{-1}) across the interface between segment n_{-1} and segment n
A_n Interfacial area (m^2) of model segment n
V_n Volume (m^2) of model segment n
z Model segment thickness (m).

The model computes vertical profiles of dissolved oxygen on an hourly basis, and operates at the same vertical scale as the thermal model. Mixing rates between layers and temperature profiles were transferred from the thermal model each time-step. A first-order, temperature-corrected deoxygenation rate, termed water column oxygen demand (WCOD), was applied to each layer to represent bulk oxygen dynamics (i.e., a combination of photosynthesis, respiration, decomposition, etc.). This rate can vary among layers depending on the light, temperature, nutrient, and other conditions that can affect the oxygen dynamics. The well-mixed epilimnion is strongly impacted by the boundary condition at the surface (described below), thus we only applied the WCOD below the thermocline, where respiration>photosynthesis. Additionally, a temporally constant areal flux is applied to the bottom segment, representing sediment oxygen demand (SOD). Table 1

Table 1
Description and source of dissolved oxygen model input and output parameters.

Parameter	Description	Spatial resolution	Source	Input/output
E	Bulk vertical dispersion coefficient (m^2 s^{-1})	Segment specific	Thermal model	Input
T	Temperature (°C)	Segment specific	Thermal model	Input
WCOD	Water column oxygen Demand (mgO$_2$ L^{-1} d^{-1})	Segment specific	Calibration	Input
SOD	Sediment oxygen demand (gO$_2$ m^{-2} d^{-1})	Bottom segment	Literature	Input
DO$_{BC}$	Dissolved oxygen boundary condition (mgO$_2$ L^{-1})	Top segment	Field data	Input
DO	Dissolved oxygen (mgO$_2$ L^{-1})	Segment specific	Calculated	Output

shows model input and output variables and their source. Fig. 4 shows a conceptual diagram of the model framework. The temperature correction to the WCOD term is illustrated below.

$$WCOD(T) = WCOD(20^{\circ}C) \cdot \theta^{T-20}$$

Where

WCOD(T) Water column oxygen demand at temperature T
WCOD(20 °C) Water column oxygen demand at temperature T = 20 °C
θ Temperature correction coefficient (1.04)
T   Temperature (°C).

Observations

Long-term (1987–2005) observations of dissolved oxygen depth profiles were compiled from several stations in the Central Basin of Lake Erie. These data were obtained from several sources, including Great Lakes National Program Office (GLNPO), National Water Research Institute of Environment Canada (NWRI), and the International Field Years on Lake Erie Program (IFYLE, 2006).

Boundary conditions were set at the water surface based on observations and linear interpolation across sampling times. The data provide roughly distinct profiles from six to ten stations during each cruise throughout each year. Reported SOD values have not varied significantly over the time period of the model, so we used a value of 0.7 gO$_2$ m^{-2} d^{-1} (Matisoff and Neeson, 2005; Schloesser et al., 2005; Snodgrass, 1987; Snodgrass and Fay, 1987), corrected for differences from a base temperature (20 °C) using an Arrhenius function similar to that of the WCOD described previously.

Charlton (1980a) found that hypolimnetic oxygen concentrations in Lake Erie generally decreased linearly with time during the 1950s–1970s, resulting in a constant depletion rate for each year. More recent studies of the depletion rates (Burns et al., 2005; Rosa and Burns, 1987) report single annual values, based on calculated differences between seasonally averaged observations; however, they note that seasonal production, especially at the thermocline, can significantly affect the oxygen dynamics. While our dynamic model allows for within year

variation in WCOD values, the variability in oxygen depletion is most likely a result of nutrient cycling and biological processes, and because these dynamics are not explicitly modeled, varying the WCOD on a daily basis would result in essentially a curve-fitting exercise. Instead, by using a constant hypolimnetic WCOD rate throughout the year, one can assess how well the model captures the oxygen dynamics as a function of seasonal changes in the hydrodynamic effects only. That is, if the model can capture the dissolved oxygen profiles without varying the annual-average WCOD across years, then the mixing and thermal regime would be much more significant in determining the extent of hypoxia, compared to biological process.

Results

Thermal model results

For model validation we selected two periods with observations, 2004 and 2005. During these and other modeled years (1988–2005) we used the same coefficient values obtained in the 1994 calibration. The 2005 dataset was considerably more complete (see Rao et al., 2008 for details of observation campaign), therefore we restrict our model validation discussion primarily to 2005 (Fig. 5). Overall, the 1D model accurately described the onset of stratification and thermocline development in summer. Most problems occurred in late August and early September, when the model underestimated the sudden increase in mixed layer depth caused by storms on days 242 and 272. The latter storm almost totally eliminated thermocline which did not occur in the model run until around day 298. A similar problem occurred in the model in 2004, and we attribute this to 3D effects not represented in the 1D model, such as horizontal advection and internal wave propagation.

As in the 1994 calibration, maximum model errors (RMSE) in 2005 occurred in the thermocline, at and below 15 m (Fig. 3). Model errors were higher in 2005 than in 1994 (between 1.2 and 3.9 °C), most probably due to the more complete thermocline observations in 2005. The magnitude of errors is comparable but somewhat higher than found in other recent (although 3D) modeling studies of Lake Michigan (Beletsky and Schwab, 2001) and Lake Ontario (Huang et al., 2010) which reported RMSE up to 2.5 °C. In addition to the 3D effects, higher errors can be also attributed to a particularly sharp
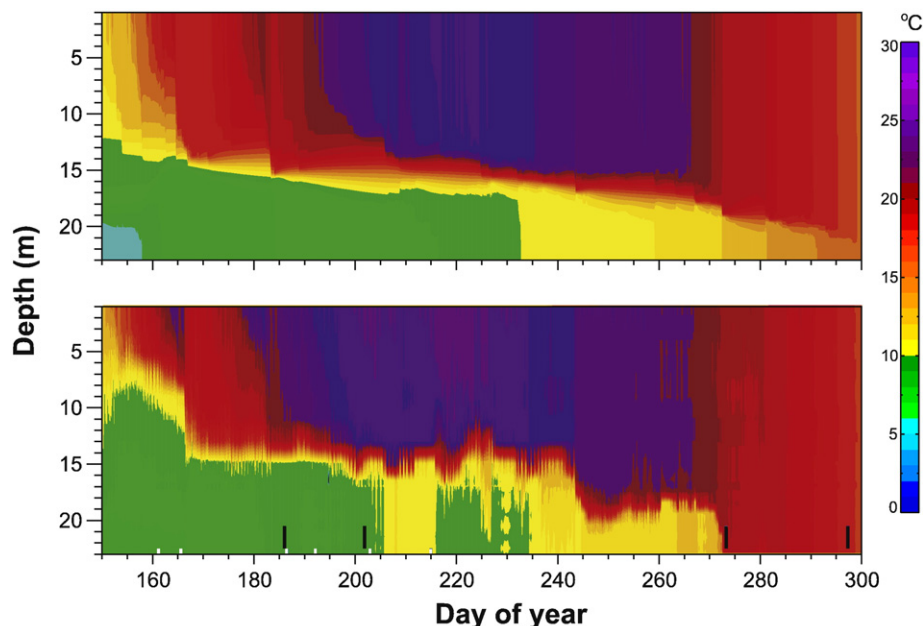

Fig. 5. Modeled (upper panel) versus observed (lower panel) temperature in central Lake Erie in 2005.
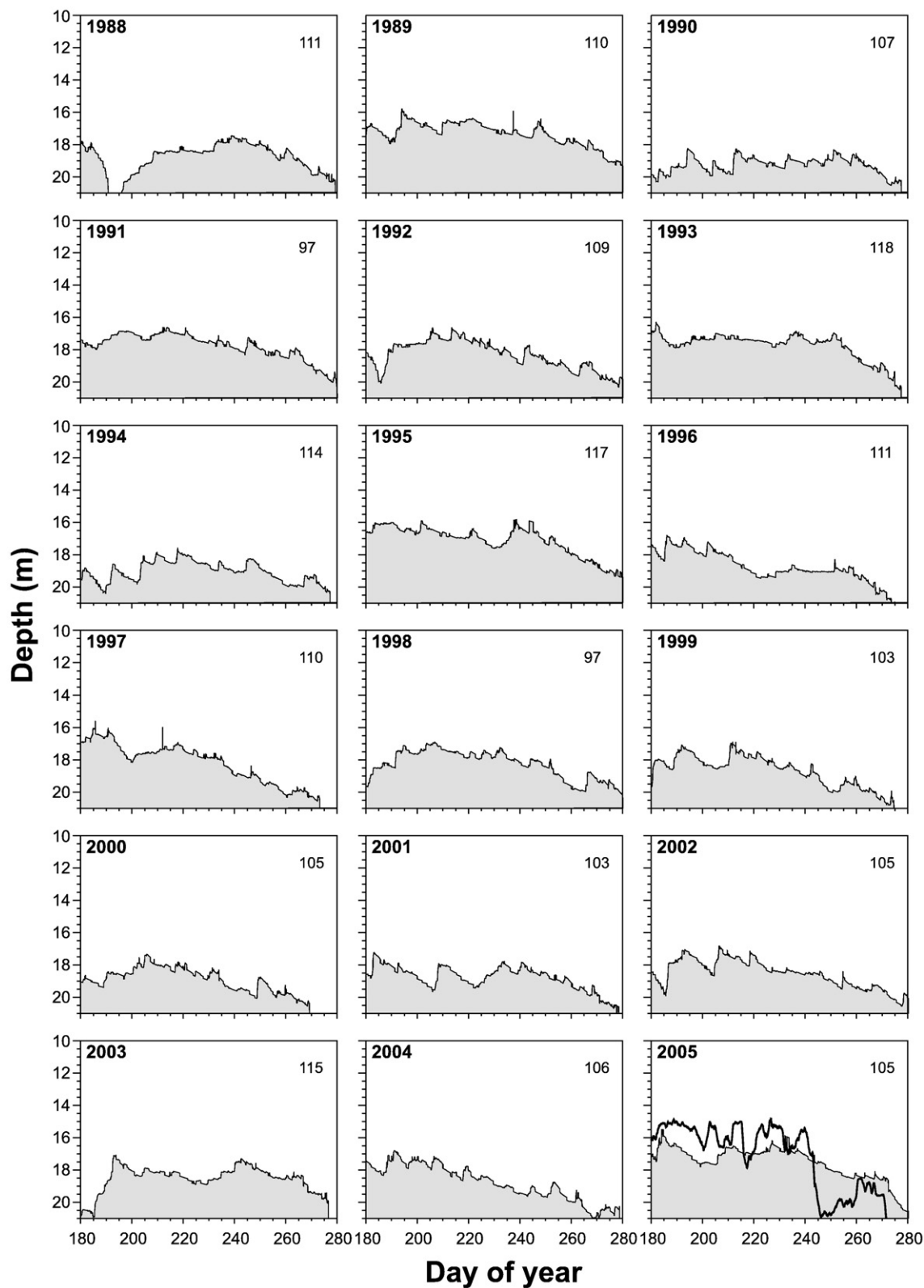
Fig. 6. Modeled hypolimnion thickness in 1988–2005 (bottom 3 meters are not shown). The number in the upper right corner is the day of stratification onset. The 2005 panel also shows observed (18-hr smoothed) hypolimnion thickness (black line).

thermocline developing in Lake Erie by the end of summer (Schertzer et al., 1987).

Additional model validation is presented in Fig. 6 which shows comparison of modeled and observed hypolimnion depth in 2005. To identify the mixed layer, thermocline, and hypolimnion depths more

objectively, each vertical temperature profile (both modeled and observed) was approximated (in a least squares sense) with a 3-layer structure with uniform temperature in the top and bottom layers, and a linear temperature decrease between the top and bottom layers. The model generated a deeper than observed thermocline during July and
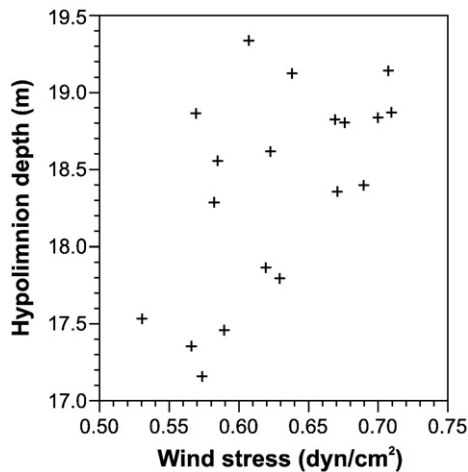
Fig. 7. Scatter plot of average hypolimnion depth (m) versus average wind stress (dyne/cm²) in 1987–2005.

August but (as mentioned above) underestimated the 5 m decrease in hypolimnion thickness due to storm on day 242. In the model results, this decrease is less than 1 m (seen in Fig. 5). The hypolimnion recovered somewhat by day 260 when the model started matching observations until another storm on day 272. The model did simulate a deeper hypolimnion (by about 2 m) in 2004 versus 2005 observed by Rao et al. (2008).

Fig. 6 also shows inter-annual variability of hypolimnion depth for other modeled spring–summer–fall periods in 1988–2005. Since we did not simulated ice cover, the model was initialized with vertically uniform temperature based on cruise observations made between April 1 and April 25 each year. Initial water temperature in early spring varied substantially between years, i.e. it was about 1 °C in 1994 after the cold 1993–1994 winter to slightly over 4 °C in 1998 after the exceptionally warm winter of 1997–1998. This affects the onset of stratification (day when lake surface temperature becomes higher than 4 °C), which varied by about 3 weeks, from day 97 to day 118 (Fig. 6).

Inter-annual variability of mean hypolimnion depth (which varied between 17.2 and 19.3 m depths) is clearly pronounced in model results (Fig. 6) with years 1989, 1995 and 2005 exhibiting thick hypolimnia, while 1990 and 1994 showed thin hypolimnia. This is

mostly related to inter-annual variability of wind stress (which varied between 0.53 and 0.71 dynes/cm²) because higher wind stress leads to more mixing and hence a deeper (i.e., thinner) hypolimnion (Fig. 7). We found dependence of hypolimnion depth on the net heat flux (which varied between 17 and 52 W/m²) less revealing since the latter itself correlates with wind speed (via latent and sensible heat flux components). We did not find any significant correlations between temperature gradient in the thermocline (between 1.6 and 2.6 °C/m) and either wind stress or heat flux. At the same time, there is a clear link between air temperature and lake surface temperature, both changing with similar amplitude (between 20.0 and 21.4 °C and between 21.3 and 22.9 °C respectively).

Dissolved oxygen model results

The model was calibrated for 1987–2005 by varying the hypolimnetic WCOD values to match the observed timing of the onset of hypoxia. WCOD values were held constant throughout the year, but varied across years to provide the best match to intra-annual variations in dissolved oxygen concentrations , and then to explore if and how WCOD varied among years. Observed oxygen vertical profiles were also used to guide the calibration. An example of model output is shown in Fig. 8. The magnitude and timing of the oxygen minima are also captured well. There are small scale changes in observations (e.g., in mid-July) that the model does not capture, and these coincide with the limitations of the thermal model in capturing fluctuations at the thermocline (Fig. 5). These fluctuations in the oxygen conditions are consistent with the storm episode disruptions detailed by Lam et al. (1987) and demonstrate a limitation of the 1D model framework.

To illustrate long-term model performance, average modeled hypolimnetic DO concentration is compared to average observations below the thermocline (Figs. 9–11). Because the model boundary condition is specified at the surface, the epilimnion model averages match the observations very well. Overall, the model performs well in capturing the temporal profiles for most years. Again, small scale fluctuations in the observed dissolved oxygen concentration are not captured well, as the model assumes a constant loss rate throughout a given year. To demonstrate the sensitivity to the calibrated WCOD term, we also show model results using upper and lower bounds corresponding to the range of calibrated annual-average WCOD values (1 and 0.001 mg L^{-1} d^{-1}, respectively).
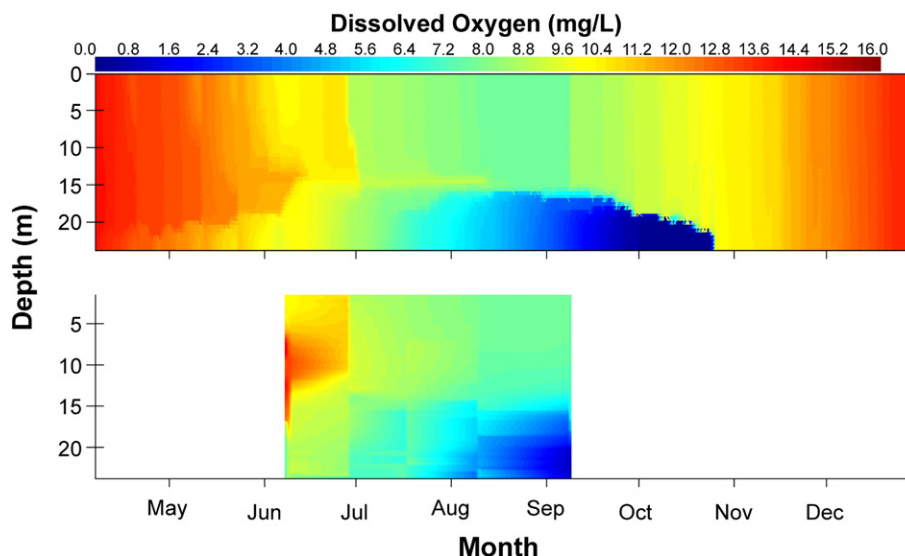

Fig. 8. Calibrated dissolved oxygen model results for 2005. Model output shown in upper panel, observations in bottom panel, when data are present.
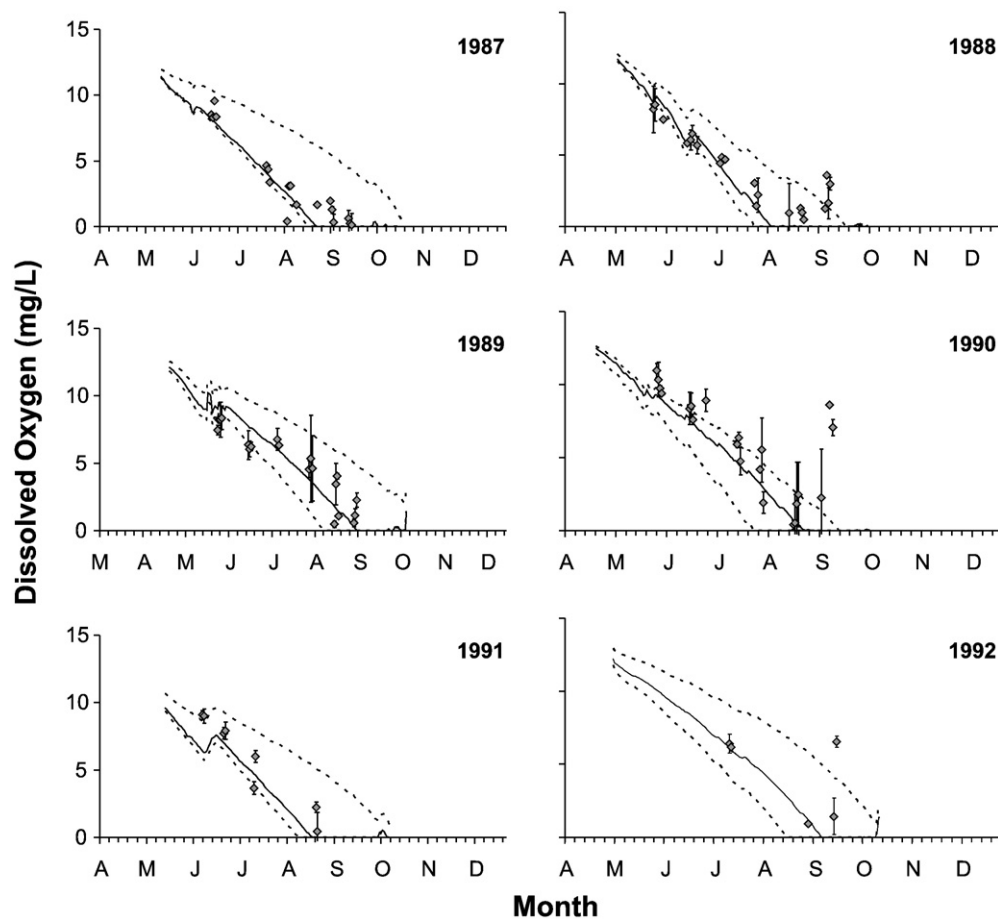
Fig. 9. Calibrated dissolved oxygen model results averaged over hypolimnion (1987–1992). Model shown as black solid line, data ($+/-1$ s.d.) shown as gray diamonds, and results using upper and lower bounds of WCOD shown as black dotted lines.

Discussion

Our primary objective was to test the hypothesis that climate-driven variability in thermal structure and mixing alone could explain the inter-annual variability and trend in hypolimnetic oxygen depletion rates. For this to be the case there would be no need to vary WCOD across years. However, to reproduce those depletion rates we had to vary WCOD (Fig. 12), and we therefore reject the hypothesis that variation in thermal structure alone controlled changes in hypoxia.

We combined our sediment oxygen demand and water column demand (WCOD) resulting from our calibration to compare our model-derived total hypolimnetic volumetric oxygen demand (HVOD) with observed rates that were estimated by slopes of linear regressions through hypolimnetic oxygen time-series . The model-estimated rates compare well with those based on observations (Fig. 13). Fig. 13 also includes the HVOD rates that would result by using the minimum and maximum hypolimnetic WCOD rates as constants (dotted lines), and further demonstrates the variability required to match observations.

To test this more explicitly, we explored relationships between the oxygen depletion rate and initial thermocline depth and between the oxygen depletion rate and date of onset of thermal stratification and found little correlation ($r = 0.17$ and 0.46, respectively). So, while these factors can contribute to the magnitude of hypoxia, the relative influence on inter-annual variability appears to be small compared to differences in biological productivity.

The calibrated WCOD values decreased significantly between 1987 and 1996, and then increased through 2005. This implies that eutrophication processes contributing to hypoxia (i.e., generation of organic matter in the water column) had declined up to 1994, but are

increasing in recent years. Soluble reactive phosphorus loading to the western and central basins (Richards, 2006) followed a similar trend (Fig. 14) post 1993; however total phosphorus does not follow the same trend. A regression of WCOD versus the corresponding annual SRP load in the post-1993 period resulted in a correlation coefficient of 0.70, while a regression with annual total phosphorus load (Dolan, 1993; Dolan and McGunagle, 2005) yielded only a correlation coefficient of 0.11 (using the load from the previous year resulted in a slightly better correlation of 0.20). Further supporting the notion that oxygen demand is correlated with biological productivity, a regression between the WCOD and average in lake chlorophyll-a concentration yielded a correlation coefficient of 0.41.

Rosa and Burns (1987), Burns et al. (2005), and Charlton (1980a) estimated a similar HVOD term for Lake Erie in previous works based on the rate of change in observed data. Those works did not account for vertical variations in dissolved oxygen data, were not as temporally resolved, and did not explicitly incorporate the physical mixing of the system. Despite the different methodologies, our estimates when combined with SOD are similar to theirs. The previous studies used data dating back to the 1929 (sporadic years from 1948 to 1979 and 1980 to 2002), and the HVOD values obtained were in the 2 to 4 $g/m^3/mo$ range, however, our values are in the 1 to 2 $g/m^3/mo$ range, post-1993.

The HVOD term incorporates the oxygen demand associated with the deposition of organic matter to the sediments, which represents a significant portion of the total oxygen depletion. Because the SOD is large and does not change dramatically over our period of analysis, it masks annual variability in HVOD. SOD represents 63% of the HVOD on average in our analysis. The relative contribution is much lower in earlier years because WCOD values are higher before 1994. Our
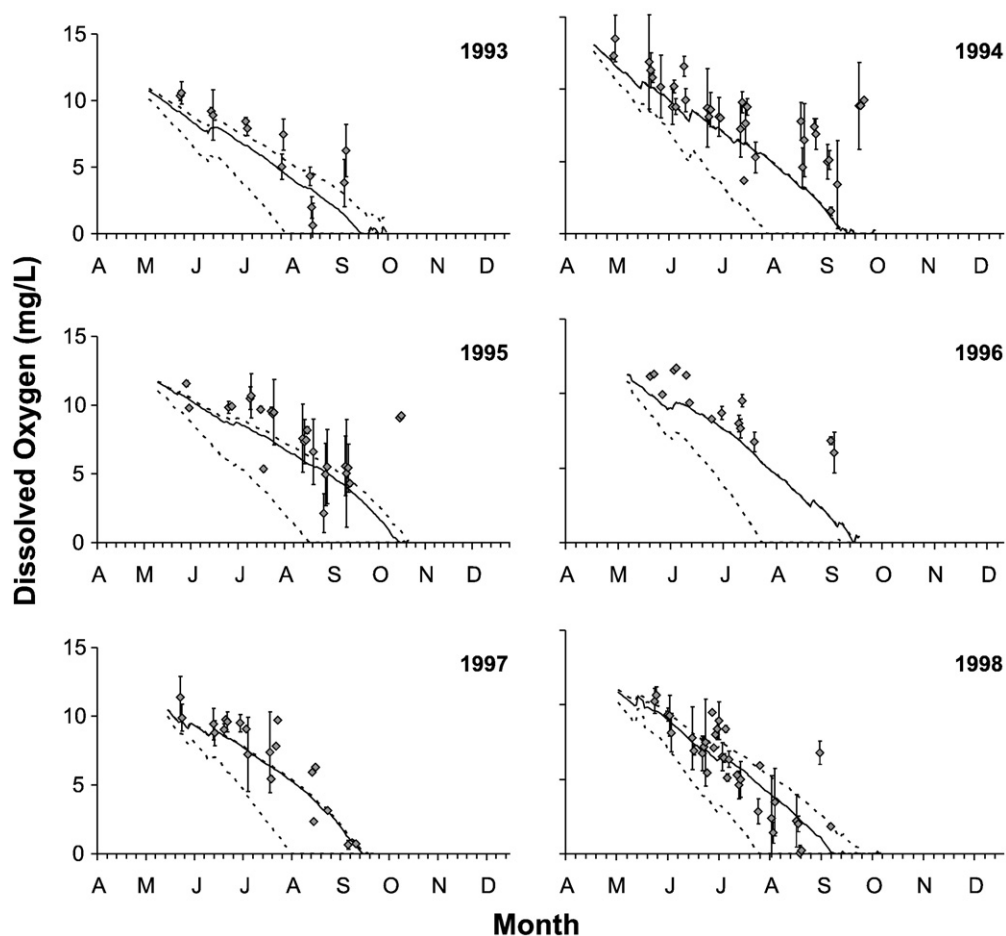
Fig. 10. Calibrated dissolved oxygen model results averaged over hypolimnion (1993–1998). Model shown as black solid line, data (+/−1 s.d.) shown as gray diamonds, and results using upper and lower bounds of WCOD shown as black dotted lines.

modeling analysis isolates the water column oxygen demand, and better represents the seasonal oxygen dynamics. By isolating the water column depletion from the bulk hypolimnetic depletion, we can better distinguish changes in the oxygen dynamics, as the biologic processes in the water column vary more rapidly than in the sediments.

It should be noted, however, that there are other important characteristics of hypoxia other than the depletion rate (including spatial extent, volume, and duration) that are not examined here. These factors may be more significantly linked to the physical and morphologic conditions in the lake; however, we cannot appropriately quantify this with a 1-dimensional model of this complexity.

Conclusions

A one-dimensional, coupled, thermal dynamics-dissolved oxygen model was driven by realistic, climate-driven physics and calibrated and applied for 1987–2005. The dissolved oxygen component was calibrated to seasonal oxygen concentrations by adjusting only the water column oxygen demand (WCOD) term for each year, with the goal of focusing on the impact of the lake's thermal structure on oxygen resources. If it were possible to match observations in all years using a single value for WCOD, the role of the thermal structure could be considered to be the dominant forcing. However, using reasonable upper and lower bounds for WCOD in sensitivity runs demonstrated that the model did not perform well unless WCOD was adjusted year by year; in fact, WCOD shifted from one extreme to the other (Figs. 9–11).

Our analysis indicates that water column oxygen demand in the Central Basin of Lake Erie changed significantly between 1987 and 2005, with higher depletion rates early, declining to a minimum in 1993, followed by an increase from 1994 to 2005 (Fig. 13). The initial thermocline depth at the onset of stratification varied between 17 and 20 m, but did not follow a similar trend and was not significantly correlated with the depletion rate. Similarly, WCOD was not significantly correlated with average hypolimnetic volume. Most of the relationship between the thermal structure and oxygen depletion rate is related to the depth over which water exposed to the sediment oxygen demand is mixed. However, because the depth of the thermocline varies only approximately 2 m from year to year, this difference doesn't appear to account for the differences in total hypolimnetic oxygen demand.

In contrast, soluble reactive phosphorus loads followed a similar trend, increasing from 1994 to 2005. Richards (2006) documented the change in phosphorus loads to Lake Erie from 1980 to 2005 and showed for the four major tributaries studied, an increasing SRP loading trend since the mid-1990s, while total phosphorus load did not significantly increase in the Maumee sub-basin and increased much less than SRP, overall. Potential causes for this shift include: demographic changes, increased agricultural practices and animal density, and a possible SRP surface enrichment due to conservation tillage practices (Richards, 2006). The SRP load is more likely to directly stimulate primary production than is total phosphorus, and it was correlated with the calibrated water column oxygen demand. This suggests that changes in the characteristics of the phosphorus load and its influence on primary production, as opposed to changes in climate, are the dominant drivers of changes in hypoxia since the mid-1990s.
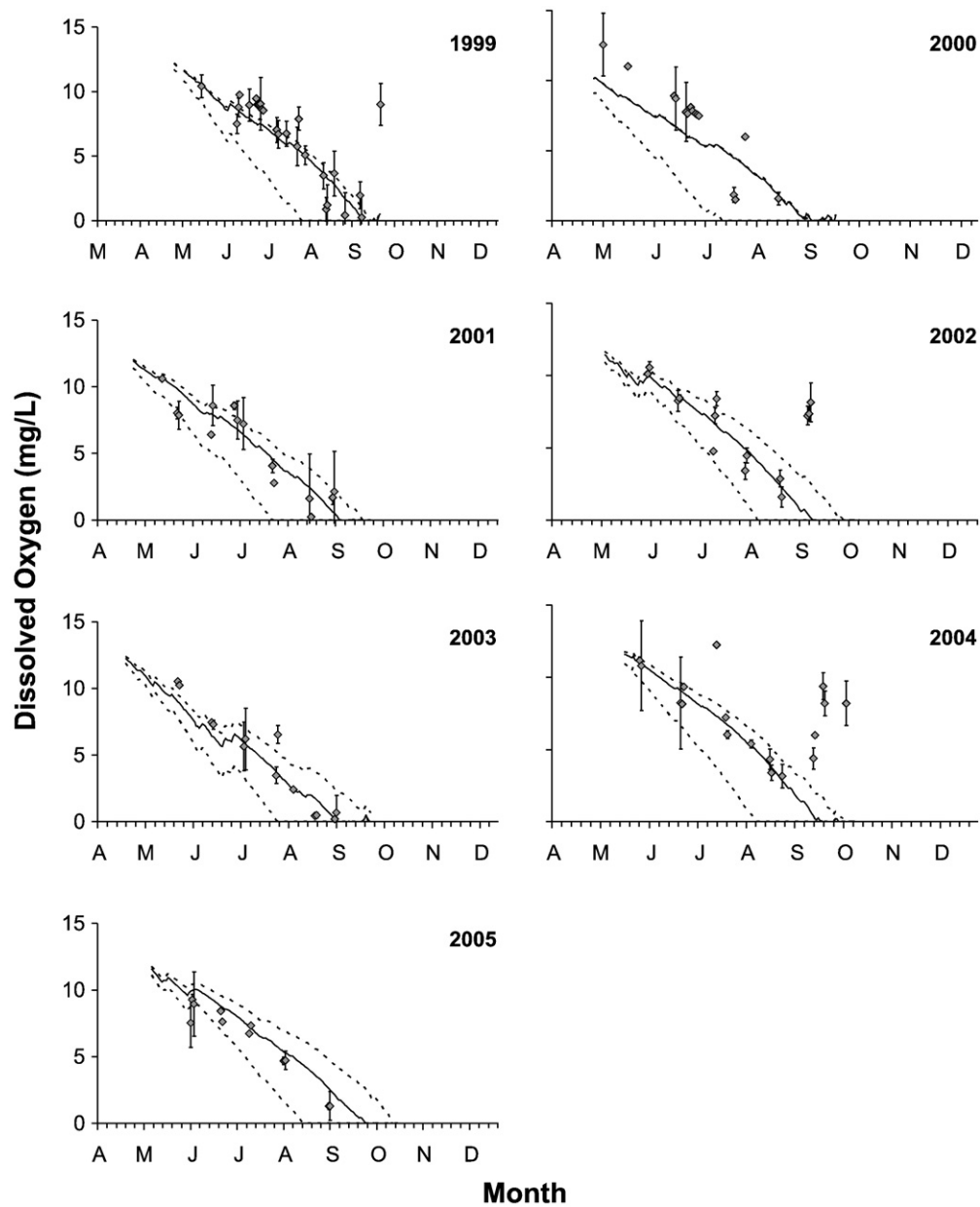
Fig. 11. Calibrated dissolved oxygen model results averaged over hypolimnion (1999–2005). Model shown as black solid line, data (+/−1 s.d.) shown as gray diamonds, and results using upper and lower bounds of WCOD shown as black dotted lines.
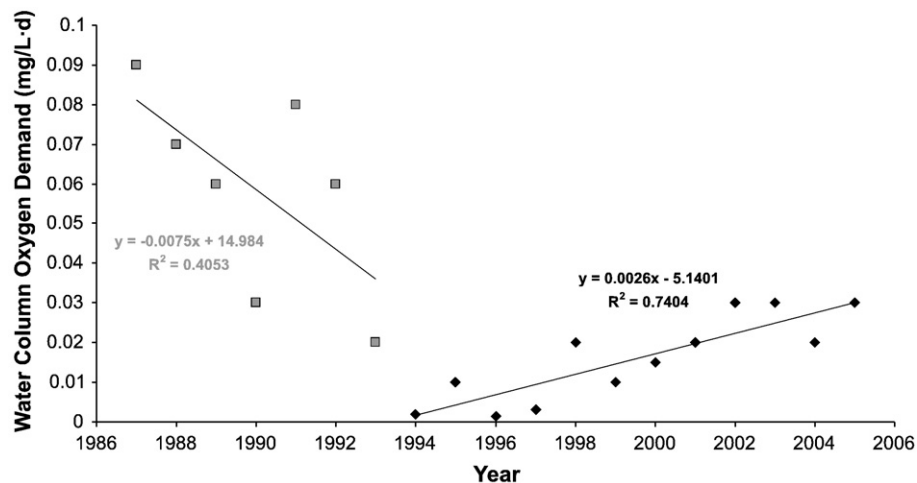

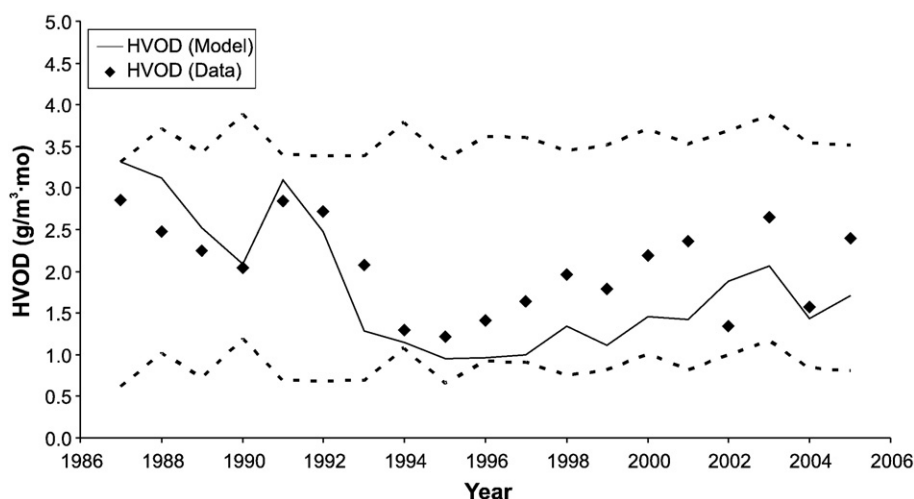Fig. 12. Calibrated WCOD rate term (1987–2005).

Fig. 13. Comparison of model-estimated HVOD from coupled thermal-dissolved oxygen model and estimated from linear regression of field data. Model-estimated HVOD rates using the upper and lower bound WCOD values are shown in dotted lines.
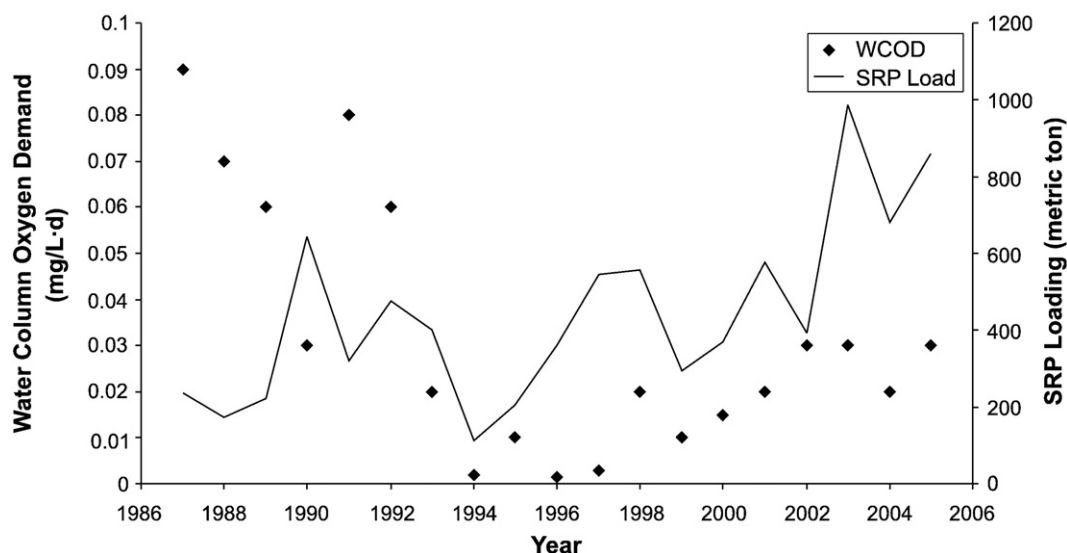

Fig. 14. Correlation between calibrated WCOD rate term and annual soluble reactive phosphorus loading.

Acknowledgments

References

Atkinson, J.F., DePinto, J.V., Lam, D.C.L., 1999. Water Quality. In: Lam, D.C.L., Schertzer, W.M. (Eds.), Chapter in: Potential Climate Change Effects on Great Lakes Hydrodynamics and Water Quality. ASCE, Reston, VA.

Bates, B.C., Kundzewicz, Z.W., Wu, S., Palutikof, J.P., 2008. Analysing regional aspects of climate change and water resources. IPCC Secretariat, Geneva.

Beletsky, D., Schwab, D.J., 2001. Modeling circulation and thermal structure in Lake Michigan: Annual cycle and interannual variability. J. Geophys. Res. 106, 19745–19771.

Bertram, P.E., 1993. Total phosphorus and dissolved oxygen trends in the central basin of Lake Erie, 1970–1991. J. Great Lakes Res. 19, 224–236.

Blumberg, A.F., Di Toro, D.M., 1990. Effects of climate warming on dissolved oxygen concentrations in Lake Erie. Trans. Am. Fish. Soc. 119, 210–223.

Blumberg, A.F., Mellor, G.L., 1987. A description of a three-dimensional coastal ocean circulation model. In: Heaps, N.S. (Ed.), In Three-Dimensional Shelf Models, Coastal and Estuarine Sciences. American Geophys. Union, pp. 1–16.

Burns, N.M., Rockwell, D.M., Bertram, P.E., Dolan, D.M., Ciborowski, J.J.H., 2005. Trends in temperature, Secchi depth, and dissolved oxygen depletion rates in the central basin of Lake Erie, 1983–2002. J. Great Lakes Res. 31, 35–49.

Charlton, M.N., 1980a. Oxygen depletion in Lake Erie: has there been any change? Can. J. Fish. Aquat. Sci. 37 (1), 72–80.

Charlton, M.N., 1980b. Hypolimnion oxygen consumption in lakes: discussion of productivity and morphometry effects. Can. J. Fish. Aquat. Sci. 37 (10), 1531–1539.

Chen, C., Ji, R., Schwab, D.J., Beletsky, D., Fahnenstiel, G.L., Jiang, M., Johengen, T.H., Vanderploeg, H., Eadie, B., Budd, J.W., Bundy, M., Gardner, W., Cotner, J., Lavrentyev, P.J., 2002. A model study of the coupled biological and physical dynamics in Lake Michigan. Ecol. Model. 152, 145–168.

Croley, T.E.I., 1990. Laurentian Great Lakes double-CO₂ climate change hydrological impacts. Climatic Change 17, 27–47.

DePinto, J.V., Young, T.C., McIlroy, M., 1986. Great Lakes water quality improvement: the strategy of phosphorus discharge control is evaluated. Environ. Sci. Technol. 20 (8), 752–759.

Di Toro, D.M., Thomas, N.A., Herdendorf, C.E., Winfield, R.P., Connolly, J.P., 1987. a post audit of a Lake Erie eutrophication model. J. Great Lakes Res. 13, 801–825.

Diaz, R.J., 2001. Overview of hypoxia around the world. J. Environ. Qual. 30, 275–281.

Dolan, D.M., 1993. Point source loadings of phosphorus to Lake Erie: 1986–1990. J. Great Lakes Res. 19, 212–223.

Dolan, D.M., McGunagle, K.P., 2005. Lake Erie total phosphorus loading analysis and update: 1996–2002. J. Great Lakes Res. 31 (Suppl. 2), 11–22.

Edwards, W.J., Conroy, J.D., Culver, D.A., 2005. Hypolimnetic Oxygen Depletion Dynamics in the Central Basin of Lake Erie. J. Great Lakes Res. 31, 262–271.

El-Shaarawi, A.H., 1987. Water Quality Changes in Lake Erie, 1968–1980. J. Great Lakes Res. 13, 674–683.

Fang, X., Stefan, H.G., 1997. Simulated climate change effects on dissolved oxygen characteristics in ice-covered lakes. Ecol. Model. 103, 209–229.

GLWQA, 1978. Great Lakes Water Quality Agreement.

Huang, A., Rao, Y.R., Lu, Y., 2010. Evaluation of a 3-D hydrodynamic model and atmospheric forecast forcing using observations in Lake Ontario. J. Geophys. Res. 115, CO2004.

IFYLE, 2006. NOAA Great Lakes Environmental Research Laboratory: International Field Years on Lake Erie (IFYLE). http://www.glerl.noaa.gov/ifyle/ 11/12/2006 2006.

Kantha, L.H., Clayson, C.A., 1994. An improved mixed layer model for geophysical applications. J. Geophys. Res. 99, 25235–25266.

Lam, D.C.L., Schertzer, W.M., 1987. Lake Erie thermocline model results: comparison with 1967–1982 data and relation to anoxic occurrences. J. Great Lakes Res. 13, 757–769.

Lam, D.C.L., Schertzer, W.M., Fraser, A.S., 1987. Oxygen depletion in Lake Erie: modeling the physical, chemical, and biological interactions, 1972 and 1979. J. Great Lakes Res. 13, 770–781.

Lehman, J.T., 2002. Mixing patterns and plankton biomass of the St. Lawrence Great Lakes under climate change scenarios. J. Great Lakes Res. 28, 583–596.

Lofgren, B.M., Quinn, F.H., Clites, A.H., Assel, R.A., Eberhardt, A.J., Luukkonen, C.L., 2002. Evaluation of potential impacts on Great Lakes water resources based on climate scenarios of two GCMs. J. Great Lakes Res. 28, 537–554.

Makarewicz, J.C., 1993. Phytoplankton biomass and species composition in Lake Erie, 1970–1987. J. Great Lakes Res. 19, 258–274.

Matisoff, G., Neeson, T.M., 2005. Oxygen concentration and demand in Lake Erie sediments. J. Great Lakes Res. 31, 284–295.

McCormick, M.J., Meadows, G.A., 1988. An intercomparison of four mixed layer models in a shallow inland sea. Journal of Geophysical Research 93 (C6), 6774–6778.

Mellor, G.L., 2001. One-dimensional, ocean surface layer modeling: a problem and a solution. J. Phys. Oceanogr. 31, 790–809.

Mellor, G.L., Blumberg, A.F., 2004. Wave breaking and ocean surface layer response. J. Phys. Oceanogr. 34, 693–698.

Mellor, G.L., Yamada, T., 1982. Development of a turbulent closure model for geophysical fluid problems. Rev. Geophys. 20, 851–875.

Paulson, C.A., Simpson, J., 1977. Irradiance measurements in the upper ocean. J. Phys. Oceanogr. 7, 952–956.

Rao, Y.R., Hawley, N., Charlton, M.N., 2008. Physical processes and hypoxia in the central basin of Lake Erie. Limnol. Oceanogr. 53, 2007–2020.

Richards, R.P., 2006. Trends in sediment and nutrients in major Lake Erie tributaries, 1975–2004. Lake Erie Lakewide Management Plan 2006 Update, p. 22.

Richards, R.P., 2002. Trends in water quality in LEASEQ rivers and streams, 1975–1995. J. Environ. Qual. 31, 90–96.

Rosa, F., Burns, N.M., 1987. Lake Erie Central basin oxygen depletion changes from 1929–1980. J. Great Lakes Res. 13, 684–696.

Schertzer, W.M., Saylor, J.H., Boyce, F.M., Robertson, D.G., Rosa, F., 1987. Seasonal thermal cycle of Lake Erie. J. Great Lakes Res. 13, 468–486.

Schloesser, D.W., Stickle, R.G., Bridgeman, T.B., 2005. Potential oxygen demand of sediments from Lake Erie. J. Great Lakes Res. 31, 272–283.

Schwab, D.J., Bedford, K.W., 1999. The Great Lakes forecasting system. In: Mooers, C.N.K. (Ed.), In Coastal Ocean Prediction, Coastal and Estuarine Studies. American Geophysical Union, Washington, D.C., pp. 157–173.

Snodgrass, W.J., 1987. Analysis of models and measurements for sediment oxygen demand in Lake Erie. J. Great Lakes Res. 13, 738–756.

Snodgrass, W.J., Fay, L.A., 1987. Values of sediment oxygen demand measured in the central basin of Lake Erie, 1979. J. Great Lakes Res. 13, 724–730.

Woynarovich, E., 1961. The oxygen consumption of Dreissena polymorpha (Lamellibranchiate) at different temperatures. Ann. Biol. Tihany 28, 216.